Composites Science and Technology 99 (2014) 52–58

Contents lists available at ScienceDirect

Composites Science and Technology

journal homepage: www.elsevier.com/locate/compscitech

Swellable elastomeric HNBR–MgO composite: Magnesium oxide as a novel swelling and reinforcement filler

Dingzhi Han [a], Meng Qu [b], Chee Yoon Yue [c,*], Yucun Lou [b], Simone Musso [b], Agathe Robisson [b,*]

[a] School of Materials Science and Engineering, Nanyang Technological University, Singapore 639798, Singapore
[b] Schlumberger-Doll Research, 1 Hampshire St, Cambridge, MA 02139, United States
[c] School of Mechanical and Aerospace Engineering, Nanyang Technological University, Singapore 639798, Singapore

ARTICLE INFO

Article history:
Received 10 February 2014
Received in revised form 21 April 2014
Accepted 4 May 2014
Available online 11 May 2014

Keywords:
A. Particle-reinforced composites
A. Oxides
B. Mechanical properties
C. Elastic properties
D. Dynamic mechanical thermal analysis (DMTA)

ABSTRACT

In this paper, we introduce a novel reactive rubber composite made by compounding magnesium oxide (MgO) powder with hydrogenated nitrile butadiene rubber (HNBR). This HNBR–MgO composite system initially looks and behaves like rubber, but exposure to water causes it to swell and stiffen. Compared with conventional swellable materials, which lose stiffness significantly upon swelling, the sealing capacity of these novel reactive composites improves significantly with their improved stiffness. Three mixing ratios of HNBR and MgO were examined in this study, and their properties upon reaching equilibrium in water of 82 °C were reported. The elastic modulus value tripled, reaching 80 MPa, while doubling in volume for the rubber filled with 40% by volume of MgO. After drying, modulus of this particular composite increased even further to almost 200 MPa while the volume expansion was largely retained (shrinkage of approximately 10%). In this paper, we will show that the increase in elastic modulus and volume increase are related to the reaction of MgO with water to form magnesium hydroxide, absorbing water molecules into the composite and chemically reacting with it in the process.

1. Introduction

Swellable elastomers are a class of crosslinked polymers that possess the ability to imbibe large quantities of water or oil and exhibit elasticity both before and after swelling. Their autonomous swelling is employed in a variety of applications, particularly in areas where continuous human monitoring and timely intervention is difficult or impossible. Some examples include microfluidic valves for flow control [1], self-healing cement to maintain cement integrity [2], and swell packers for sealing applications in the oilfield environment [3–6]. Unlike other applications that use only small quantities of swellable elastomers, swell packer applications involve large amounts of the elastomers corresponding to the wellbore geometries to sustain a large amount of load. Hence, the amount of swelling and mechanical properties of these materials becomes critical.

In all conventional water-swellable elastomers, and oil-swellable elastomers as well, the solvent molecules imbibed into the elastomer through osmosis interacts among themselves and with the long polymer chains mostly through Van der Waals forces and hydrogen bonding. No chemical bonding between the solvent and polymer network exists for these types of swellable materials. Therefore, the swelling is reversible when the availability of solvent changes. In addition, the swellable elastomer modulus decreases due to dilution of the stiff rubber matrix by the solvent [7,8]. All these features limit the reliability of these elastomers on long-term sealing applications in the oil field.

Using slag cement as the reactive hydrating agent, Robisson et al. [9] introduced a novel swellable elastomer that exhibits an increase in the modulus with swelling. The composite containing approximately 40 vol% slag cement swelled by approximately 25 vol% while exhibiting a threefold boost in Young's modulus. In this study, we introduce a yet different swellable elastomeric composite material that uses magnesium oxide (MgO) as filler and hydrogenated nitrile butadiene rubber (HNBR) as a matrix for improved swelling ability [10–12]. As we target sealing applications, the material should maintain high stiffness along with swelling. Our work aims at guiding material design for volume and stiffness increase optimization.

Samples with different MgO contents are studied. Volume, mass, and modulus evolutions with time exposure to water are reported. The surprisingly high swelling ability of the highly filled

* Corresponding authors. Address: Nanyang Technological University, 50 Nanyang Avenue, Singapore 639798, Singapore. Tel.: +65 6592 2696 (C.Y. Yue). Address: Schlumberger-Doll Research, 1 Hampshire St, Cambridge, MA 02139, United States. Tel.: +1 617 768 2203 (A. Robisson).
E-mail addresses: mcyyue@ntu.edu.sg (C.Y. Yue), agathe.robisson@gmail.com (A. Robisson).

http://dx.doi.org/10.1016/j.compscitech.2014.05.002
0266-3538/

composites is discussed in details, along with the mechanism behind the substantial stiffening.

2. Experimental methods

2.1. Materials used

Hydrogenated acrylonitrile butadiene rubber was chosen as the rubber matrix because it possesses good resistance to oil and fuels [13,14].

Industrial-grade dead burned MgO was purchased from Schlumberger and milled to a median size of 2 μm (D90 = 3.6 μm). The low-reactivity MgO has slow hydration kinetics, which allowed for better observation of changes occurring during the experiments. The purity of MgO was measured to be approximately 80% using X-ray fluorescence spectrometry (SPECTRO XEPOS). The remaining 20% are non-reactive components that do not participate in hydration reaction.

HNBR was compounded with different MgO concentrations (0%, 14%, 28% and 40% by volume or 0%, 34%, 55% and 67.5% by mass) to study the effect of filler content on swelling and reinforcements.

Mixing of rubber with the fillers, crosslinking co-agent, initiator, and processing aids were performed in a Banbury mixer at around 95 °C for 10 min, followed by a two-roll mill. The mixture was then cured and molded into 2-mm thick sheets in a hot press at 177 °C. Cuboidal coupon samples (with dimensions 20 mm × 4 mm × 2 mm) were cut from the sheets and used for water exposure tests.

2.2. Materials characterization

2.2.1. Mass and volume measurement

Coupon samples (20 mm × 4 mm × 2 mm) of pure HNBR and HNBR–MgO composites were immersed in deionized water at 82 °C, which is a typical downhole temperature considered for sealing applications in the oilfield. The volume and modulus changes were measured until a plateau was reached after approximately 2 months of water exposure. Three samples were tested for each time interval and their mean values with absolute deviation will be presented. However, due to the small absolute deviation observed for most experiments, the deviations may not be visible in many of the plots. In this paper, only the equilibrium values (taken after 2 months of hydration when the values stabilized) are shown and analyzed.

The samples were first removed from the water to measure their volume and modulus in the wet stage. These samples were then oven dried at 82 °C for a week to completely remove free water not chemically bonded to the MgO (complete oven drying confirmed by the negligible mass loss at 100 °C with thermogravimetric measurements). The volume and stiffness of these samples were then measured again in their dried stage.

The volume change, referred to as swelling in this work, at any given time t is defined as:

$$\text{Swelling } \% = \frac{volume_t - volume_{initial}}{volume_{initial}}, \tag{1}$$

where $volume_{initial}$ is the initial volume of sample prior to hydration and $volume_t$ is the volume of the sample at time t.

The difference between the initial mass of an unhydrated HNBR-MgO coupon sample and its mass after hydration and drying gives the mass of water that had chemically bonded to the MgO, forming magnesium hydroxide $Mg(OH)_2$, assuming no content (MgO or $Mg(OH)_2$) leaches out of the samples. The amount of MgO that had hydrated can be estimated by using Eq. (3) from the stoichiometry of Eq. (2). Furthermore, the extent of hydration of MgO, defined as the percentage of MgO that has reacted in a sample, can be obtained by using Eq. (4).

$$MgO(s) + H_2O(l) \rightarrow Mg(OH)_2(s) \tag{2}$$

$$\text{mass of reacted MgO} = \text{mass of bonded water} \times \frac{M_W \text{ of MgO}}{M_W \text{ of } H_2O} \tag{3}$$

$$\text{extent of hydration of MgO} = \frac{\text{Mass of MgO converted to } Mg(OH)_2}{\text{Original mass of MgO}} \tag{4}$$

2.2.2. Mechanical properties

Elastic (or storage) Young's moduli of the coupon samples were measured at three stages of the experiment: prior to immersing in water, immediately following its removal from water, and after subsequent oven drying for a week. The samples were tested at room temperature under uniaxial tension using a Dynamic Mechanical Analyzer (DMA Q800, TA instruments) set at 0.1% strain amplitude, 1 Hz and 125% force track. The loss modulus is found to be small (accounts for less than 6% of the normalized modulus); hence, the storage modulus alone represents the Young's modulus well. Subsequent mentions of modulus refer to Young's elastic modulus.

2.2.3. Scanning electron microscopy (SEM)

The morphology change of MgO particles in HNBR–MgO composite with hydration was investigated using a scanning electron microscope (SEM) JEOL JSM-6490LV. Cryo-microtome was employed to prepare thin slices of specimen from both initial (unhydrated) and hydrated coupon samples. Thereafter, imaging was performed on the exposed cross-sectional areas of the samples. Based on the images obtained for the composites of different filler content, the distribution of the fillers was found to be relatively homogeneous in all compounds.

The SEM was also employed to study the morphology of uncompounded MgO powder before hydration and after hydrating it for 5 days at 82 °C.

2.2.4. Transmission electron microscopy (TEM)

For a closer examination of the MgO particles and $Mg(OH)_2$ crystals formed after hydration, transmission electron microscope (TEM) JEOL 2010 was utilized to obtain high magnification images of the powdered samples as well as thin slices of the HNBR–MgO composites prepared using cryo-microtome.

2.2.5. Brunauer–Emmett–Teller method (BET)

According to previously published literature, water is first adsorbed onto the MgO surface, hydrating it by means of a dissolution process, whereby $Mg(OH)_2$ quickly reaches its saturation point (due to low solubility) and precipitates [15]. The $Mg(OH)_2$ is preferentially precipitated initially onto the MgO surface [16,17], occluding the reacting surface, and subsequently breaks off into smaller pieces due to the surface tension [18]. This breakage exposes increased fresh surfaces of the MgO for continued hydration. The specific surface area of unhydrated and hydrated MgO powder was measured using the Brunauer–Emmett–Teller (BET) nitrogen gas adsorption method (Micromeritics ASAP 2000 surface area analyzer). The change in size of the precipitates upon hydration was determined.

3. Results

3.1. Effect of MgO filler content on elastic properties

The evolution of modulus with filler content for the composites before exposure to water, after hydration (wet state) and after subsequent drying (dried state) are presented in Fig. 1. The initial

modulus increases from 3 MPa to 27 MPa when the MgO content increases from 0 to 40 vol%. In the wet state, the initial modulus increases from 3 MPa to 80 MPa, which represents reinforcement by a factor of almost 30 times. In the dried state, the initial modulus increased significantly from 3 MPa to 190 MPa, representing a reinforcement of over 60 times after water exposure and subsequent drying.

3.2. Effect of MgO filler content on swelling

It can be seen in Fig. 2a that in addition to the significant reinforcement in mechanical properties, the HNBR composite material containing 40 vol% MgO increases in volume by around 100% (in the wet state). This volume increase is largely retained after subsequent drying, where the volume increase remained at around 80% (in the dried state). Corresponding mass increases of 56% (in the wet state) and 23% (in the dried state) were obtained in these specimens (Fig. 2b).

3.3. Microstructure evolution of hydrated MgO

The morphology of free-form unhydrated and hydrated MgO was examined under the SEM. It can be seen from the micrograph (Fig. 3a) that the MgO particles exist as irregularly shaped particles with flat surfaces and sharp edges. Upon hydration, the MgO evolved into a diffused, fine structure that appears almost fluffy (Fig. 3b–d), similar to that reported elsewhere [17]. The fine particles may either be the re-precipitated $Mg(OH)_2$ after the hydration reaction or small broken bits of the original MgO particles after breakage occurred [18].

Looking at the MgO particles at higher magnification, transmission electron microscopy (TEM) images of unhydrated and hydrated MgO powder are shown in Fig. 4. These images show that the unhydrated particles (Fig. 4a and b) are in the form of well-defined crystals with a wide size distribution (between 100 and 500 nm). On the other hand, after hydrating these MgO powders, the $Mg(OH)_2$ crystals formed appear to be significantly finer (in the order of 50–100 nm) and not well formed (Fig. 4c and d). The TEM images, similar to the SEM images, showed the presence of very fine nano-sized filler particles after hydration.

BET measurement of unhydrated MgO and hydrated $Mg(OH)_2$ powders show that the specific surface area of MgO increased by a factor 10; i.e., from 4.16 m^2/g before hydration to 44.4 m^2/g after hydration. This increase in specific surface area correlates well with the finer particle size and increased complexity of particle structure of $Mg(OH)_2$ that was observed.

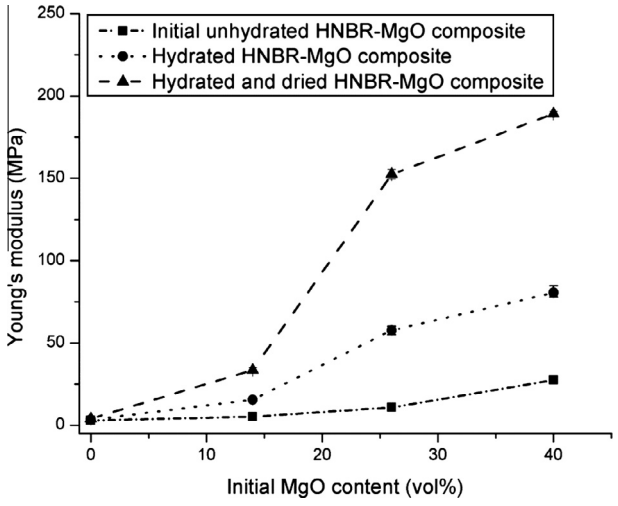

Fig. 1. Plot of change in Young's modulus of composite with MgO content and state of hydration.

Next, the morphology of MgO in the HNBR composite before and after hydration was examined. It can be seen in Fig. 5a that after compounding, the MgO in the composite has a similar shape to that of the free-form MgO filler. The MgO exists as discrete, well-distributed whitish particles within a dark-grayish rubber matrix. Moreover, the morphology of the filler in the composite that had been hydrated and then dried looks similar to that observed in Fig. 3b. After exposure to water, the filler particles appear to spread out and occupy more space in the matrix (Fig. 5b). The extent to which the rubber matrix can penetrate into the small pores created during MgO hydration will be a subject of further study. Nevertheless, it can probably be inferred from the existence of a diffused boundary between the rubber matrix and filler that some limited short-range penetration probably exists. In fact, SEM observations on compounds made of rubber and cement seemed to suggest small-scale interpenetration as well [9].

The scattered dispersion of nano-sized $Mg(OH)_2$ precipitate in the HNBR matrix was more clearly imaged using TEM. Fig. 6 shows numerous crystal-like structures that resemble those of $Mg(OH)_2$ from Fig. 4 dispersed throughout the rubber matrix. Elemental mapping of several points in Fig. 6b, including the two points marked by a white circle (●) in the blurred area and a white triangle (▲) in the defined structure area, indicated the presence of magnesium. This seems to suggest that the hydrated particles are scattered all over in the rubber matrix, which is different from the largely defined regions between particles and matrix for the initial compounds (Fig. 6a). Very fine hydrated particles with dimensions much smaller than 100 nm were observed too.

4. Analysis and discussion

4.1. Increase in mass and volume of MgO filler after hydration and drying

The earlier observations of volume and mass increase of the HNBR–MgO composite with hydration will now be considered in detail. Upon hydration, the MgO is converted into $Mg(OH)_2$ (Eq. (2)), leading to an increase in mass because water and MgO are assimilated together, and an increase in volume because the $Mg(OH)_2$ density is lower than that of MgO. Based on Eq. (2) and the theoretical values for densities of MgO (=3.19 g/cm^3) and $Mg(OH)_2$ (=2.36 g/cm^3), pure MgO has the potential to gain 45% in mass (1 mol of MgO = 40 g while 1 mol of $Mg(OH)_2$ = 58 g) and potentially gain 97% in volume (1 mol of MgO = 12.5 cm^3 while 1 mol of $Mg(OH)_2$ = 24.6 cm^3) with complete hydration.

The measured dried mass of the composites precisely follows our expectations (see Fig. 7). Indeed, the purity of MgO used is approximately 80% (see Section 2.1) and chemical reaction predicts an increase of 45% in the mass of pure MgO. Thus, the HNBR–MgO-40 composite specimen that initially comprises 67.5% MgO by mass is expected to show an increase in mass of $0.45 \times 0.8 \times 0.675 = 24\%$. Experimental results show an increase in mass of 23%, which is in agreement with the theoretical prediction. This also confirms that almost 100% of the MgO content of the MgO powder had been hydrated. It should be noted that the mass and volume increases of HNBR–MgO composites with hydration are only attributed to MgO hydration because swelling of pure HNBR is negligible (see Fig. 2).

On the other hand, the volume increase was found to be much higher than our expectation (Fig. 7b). For example, the HNBR–MgO-40 sample is expected to have an increase in volume of 0.97 (theoretical volume increase) × 0.8 (MgO content in

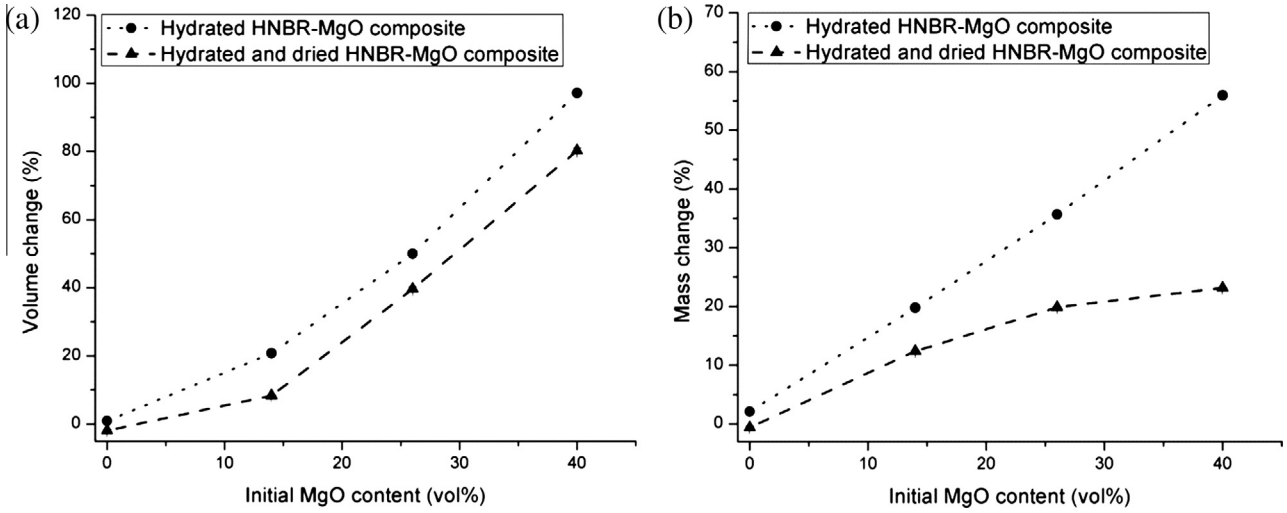

Fig. 2. Plot of change in extent of (a) composite swelling and (b) composite mass change, with MgO filler content of composites.

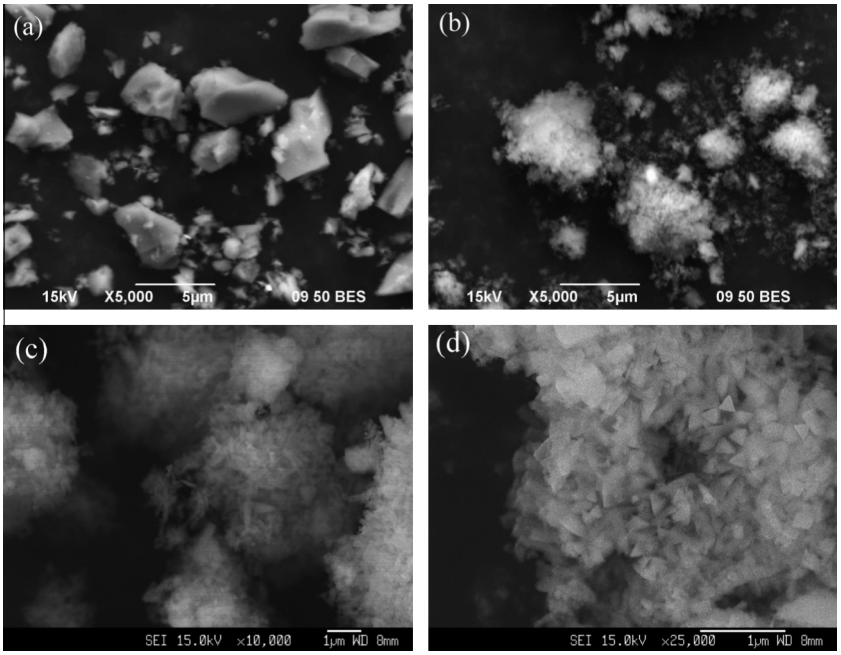

Fig. 3. Typical backscattered micrographs of (a) MgO and (b) $Mg(OH)_2$. Secondary electron imaging of $Mg(OH)_2$ at (c) 10,000 magnification and (d) 25,000 magnification. The white particles are the MgO and $Mg(OH)_2$ powder while the black areas are the background.

filler) × 0.4 (filler content in composite) = 31%, which is significantly lower than the measured volume increase of about 80%. This result indicates that the MgO volume swelled 250% (=0.8/0.8/0.4) instead of the theoretical 97%; hence, the density of $Mg(OH)_2$ in the hydrated HNBR–MgO-40 that has been dried is approximately 1.3 g/cm^3 (instead of 2.36 g/cm^3). One of the possible reasons for this low density is that fine precipitates aggregate to form a porous structure, similar to the morphology shown in Fig. 3, which may trap more voids, or micro-porosities, with increasing connectivity of the fillers as filler content increases. The porosity of $Mg(OH)_2$ in HNBR–MgO-40 is calculated to be approximately 40%. The same calculation can be repeated for the two other samples (Fig. 8) and the porosity of $Mg(OH)_2$ in the HNBR–MgO-26 and HNBR–MgO-14 specimens are about 28.5% and 2.5%, respectively.

It is important to note that cross-linked rubber matrix has the ability to relax and close any possible voids or tears formed within, particularly at the elevated drying temperature of 82 °C. On the other hand, the filler network is stiff and will not collapse completely upon drying. Therefore, any voids present in the composite most likely reside within the fillers.

It is worth mentioning that in the hydrated state prior to drying, the samples are additionally swollen by 10–20% in volume, while the mass is much higher (60% higher for HNBR–MgO-14 and 140% higher for HNBR–MgO-40). In other words, much more water than necessary enters the composites (probably due to high-osmotic pressure driven by Mg^{2+} and OH^- ions), and the fillers are stiff enough (while porous) to not fully collapse upon drying.

4.2. Modulus evolution as a function of real filler content

The increase in modulus with initial MgO filler content was shown previously in Fig. 1; however, the actual filler content

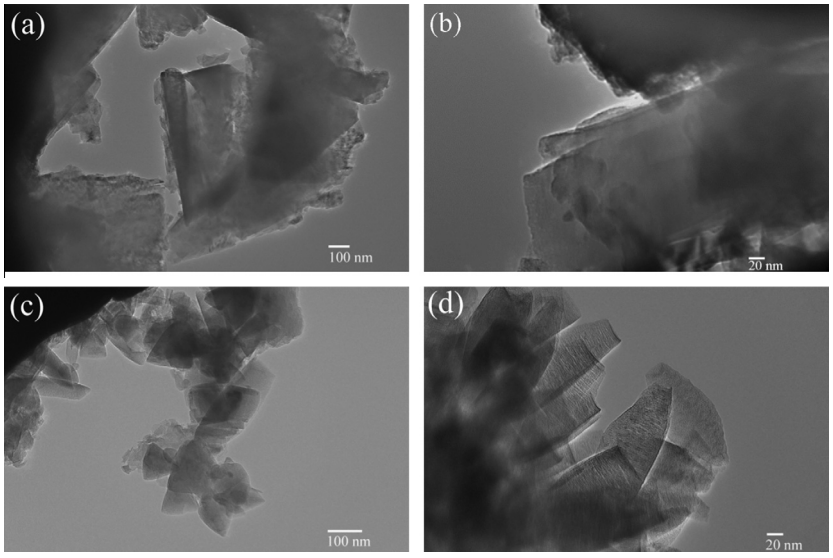

Fig. 4. Typical TEM images of (a) MgO at 15,000× magnification, (b) MgO at 60,000 magnification, (c) $Mg(OH)_2$ at 25,000× magnification and (d) $Mg(OH)_2$ at 50,000× magnification.

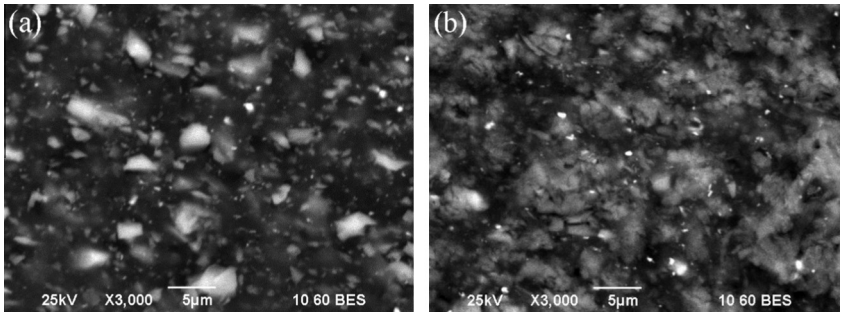

Fig. 5. Typical backscattered electron micrographs of (a) unhydrated and (b) hydrated HNBR–MgO compounds filled with 14% by volume of MgO. The whittish-gray areas in lighter shades represent the MgO and $Mg(OH)_2$ particles while the darker background represent the HNBR matrix .

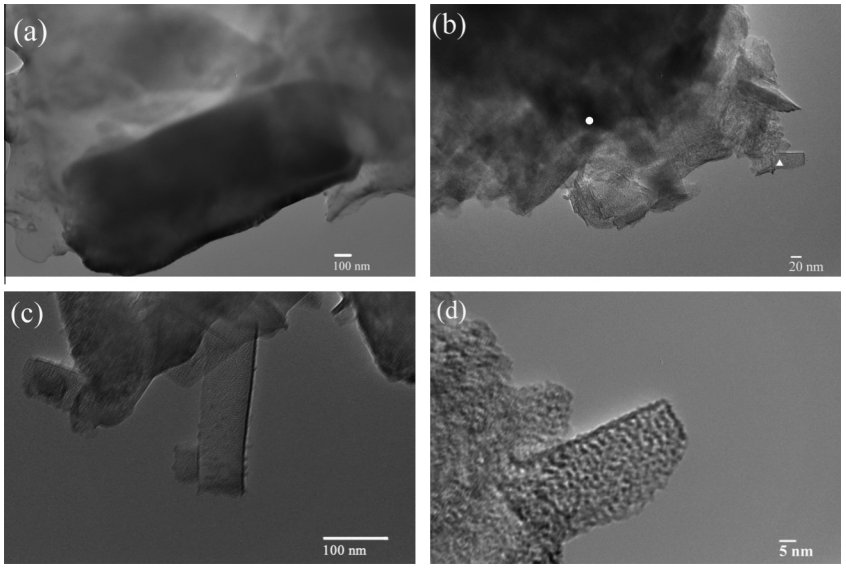

Fig. 6. Typical TEM images of (a) unhydrated composite at 12,000× magnification, (b) hydrated composite at 40,000× magnification, (c) hydrated composite at 30,000× magnification and (d) hydrated composite at 250,000× magnification. These images were obtained using HNBR–MgO composite filled with 40% by volume MgO.

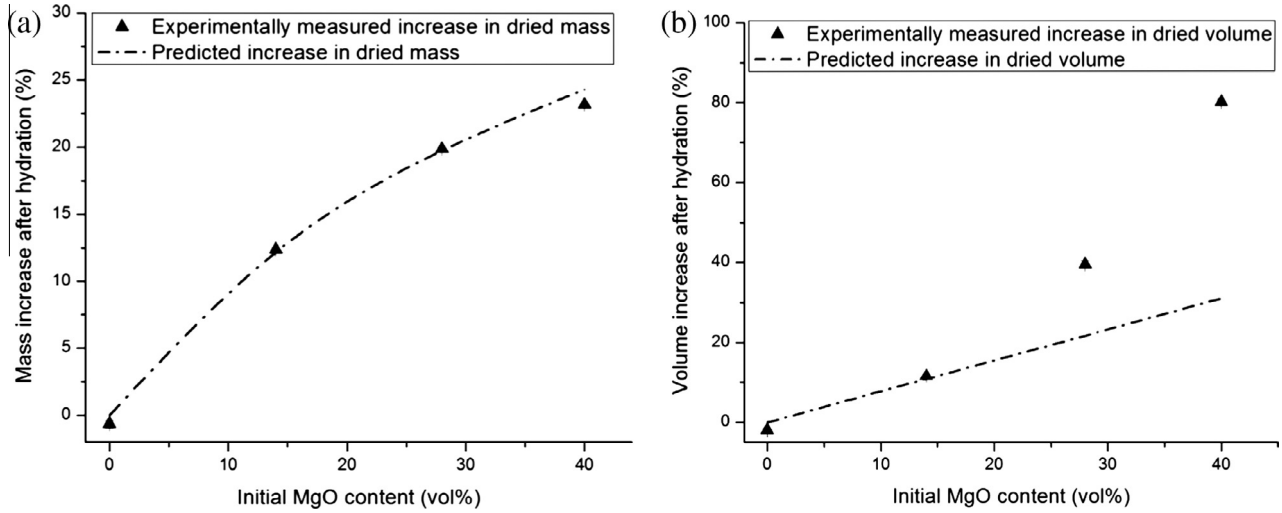

Fig. 7. Plot of change in (a) actual and predicted mass increase and (b) actual and predicted volume increase for samples that have been hydrated (assuming full hydration of MgO into $Mg(OH)_2$) and dried fully.

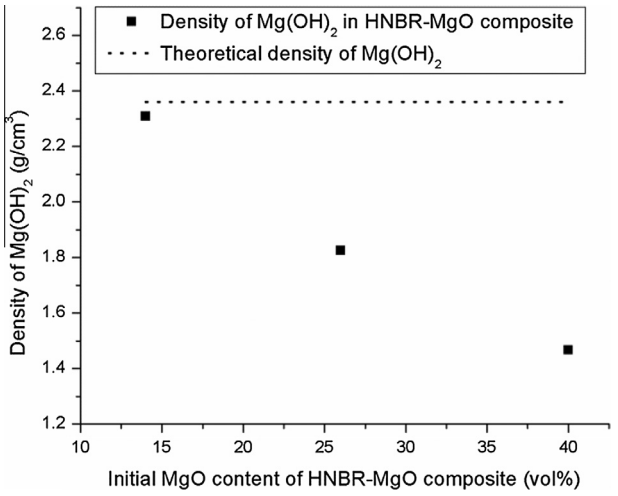

Fig. 8. Measured and theoretical densities of $Mg(OH)_2$ of dried HNBR–MgO composite (the measured density was calculated from volume and mass changes assuming all changes took place in the filler hydrates and not in the rubber matrix).

($MgO + Mg(OH)_2$) of the composites also increases with hydration. This increase in filler content undoubtedly increases the matrix stiffness. To properly evaluate the contribution of filler content in relation to the modulus increase with hydration, Fig. 1 can be re-plotted with actual filler content of the samples after hydration.

As discussed previously in Section 4.1, the change in volume of the composites is mainly attributed to the fillers. Therefore, the actual filler volume fraction (v_f) in the HNBR–MgO composite after hydration, taking into account both the MgO and $Mg(OH)_2$ as solid fillers, is defined as:

$$v_f = \frac{\text{volume}_{\text{MgO}} + \text{volume}_{\text{Mg(OH)}_2}}{\text{total volume of sample}} \tag{5}$$

Filler content of dried hydrated composite

$$= \frac{vol_{dried\ comp} - vol_{matrix}}{vol_{dried\ comp}} \tag{6}$$

Filler content of wet hydrated composite

$$= \frac{vol_{dried\ comp} - vol_{matrix}}{vol_{wet\ comp}} \tag{7}$$

$$vol_{matrix} = (1 - v_{f_{initial}}) \times vol_{ini}, \tag{8}$$

where $v_{finitial}$ is the initial filler content of the samples, vol_{ini} is the initial sample volume before hydration, vol_{matrix} is the volume of HNBR matrix that does not change with hydration, $vol_{dried\ comp}$ is the sample volume after hydration and drying in an oven, and $vol_{wet\ comp}$ is the sample volume after hydration but before drying.

Based on the above considerations, the filler content was found to increase from the initial values of 14 vol%, 28 vol%, and 40 vol% to 21 vol%, 44 vol%, and 60 vol%, respectively after hydration; and then to 24 vol%, 49 vol%, and 67 vol% after subsequent drying for a week in an oven at 82 °C whereupon the unbounded water had completely been driven off. The modulus of the composite at each of these points is shown in Fig. 9 with a polynomial line fitting the points of the same state (initial, hydrated, or hydrated and dried) using the least-squares method.

If the increase in filler content is the only factor causing the modulus increase with hydration, all three curves in Fig. 9 should coincide on the same line [21,22]. However, for the same filler content, the modulus of the hydrated samples before drying appears to be greater than that of the initial samples. Moreover, the modulus of the hydrated and dried samples is even higher than that of the

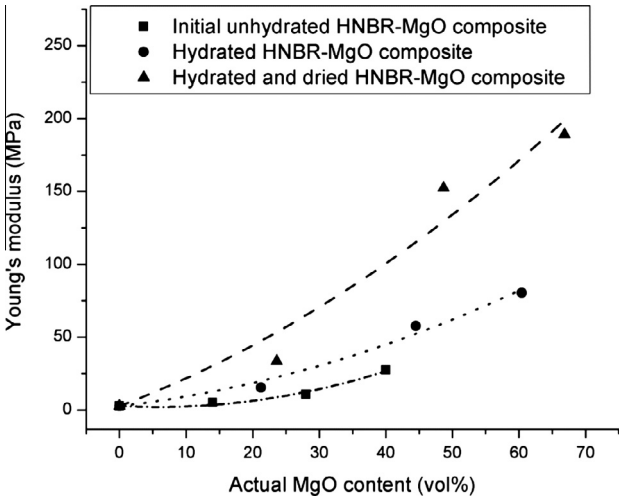

Fig. 9. Comparison of HNBR–MgO composite Young's modulus in different states.

hydrated samples before drying. It is also important to note that the modulus of the $Mg(OH)_2$ is lower than that of MgO [19,20], and even more so since $Mg(OH)_2$ is highly porous in the composites, as discussed before. Although the rule of mixture for composites asserts that the modulus of the hydrated composite should be lower than before hydration, the opposite was observed. This result strongly indicated that there are other important factors affecting the modulus and mechanical properties of such HNBR–MgO composites.

A factor contributing to these results may be the change in filler particle size and morphology or structure after hydration, as was mentioned in Section 3.3. It is apparent that the micro-sized MgO fillers converted into nano-sized $Mg(OH)_2$ fillers upon hydration. The finer nano-sized filler particles will have much higher contact surface area with the HNBR matrix, which may lead to the modulus increase.

5. Conclusions

In this study, swelling (up to $\approx$ 100%) and stiffening (up to $\approx$ 200% increase in modulus) of the novel HNBR–MgO reactive composite was observed. This new swellable elastomeric composite system can be used for sealing applications. By tuning the filler content, both swelling and elastic properties can be significantly improved. Increasing the filler volume percent from 14% to 40% results in a fourfold improvement in the swelling ratio and hydrated storage modulus of the composites. This result shows the possibility for a broad application of these novel reactive composites, especially where good mechanical properties are needed.

We studied the swelling mechanism and mechanism of modulus evolution of this novel composite. Swelling of wet hydrated composites is due to the chemically bound water in $Mg(OH)_2$ and free water. After drying, free water was removed but micro-porosities in $Mg(OH)_2$ fillers where the free water resided remained, giving retained swelling (or irreversible swelling) that was higher than expected.

Reinforcement with swelling is attributed to two main mechanisms. The first of these mechanisms is the increased volume fraction of stiff fillers with hydration, while the second mechanism is the increased specific surface area of the hydration product that leads to greater contact with the rubber matrix. A study of the transient dynamics of swelling and reinforcement, as well as the effect of filler network and porosity on the mechanical properties of these composites, is currently underway. Large deformation tensile tests of these composites and a numerical model to relate the change in modulus to filler content are other areas of study that the authors intend to pursue. This work can also be extended to the study of other reactive composite systems.

Acknowledgements

The authors would like to thank Schlumberger for its support and permission to publish.

References

[1] Beebe DJ, Moore JS, Bauer JM, Yu Q, Liu RH, Devadoss C, et al. Functional hydrogel structures for autonomous flow control inside microfluidic channels. Nature 2000;404(6778):588–90.
[2] Cavanagh PH, Johnson CR, Roy-Delage SL, DeBruijn GG, Cooper I, Guillot DJ, et al. Self-healing cement – novel technology to achieve leak-free wells. In: SPE/IADC drilling conference, Amsterdam, The Netherlands: SPE/IADC drilling conference; 2007.
[3] Laws MS, Fraser JE, Soek H, Carter N. PDOB's proactive approach to solving a zonal isolation challenge in Harweel HP wells using swell packers. IADC/SPE Asia Pacific drilling technology conference and exhibition, Bangkok, Thailand: Society of Petroleum Engineers; 2006.
[4] Brooks B, Davis T, DeLucia F. Use of swellable elastomers to enhance cementation in deep water applications. In: Deep offshore technology conference – international, Houston, TX; 2008.
[5] Yakeley S, Foster T, Laflin WJ. Swellable packers for well fracturing and stimulation. In: SPE annual technical conference and exhibition, Anaheim, California, U.S.A.: Society of Petroleum Engineers; 2007.
[6] McElfresh P, Guo L. Studies of water swellable NBR for downhole sealing applications. Rubber World: Rubber World 2008.
[7] Peng HT, Martineau L, Shek PN. Hydrogel–elastomer composite biomaterials. 1. Preparation of interpenetrating polymer networks and in vitro characterization of swelling stability and mechanical properties. J Mater Sci Mater Med 2007;18(6):975–86.
[8] Rubinstein M, Colby RH, Dobrynin AV, Joanny J-F. Elastic modulus and equilibrium swelling of polyelectrolyte gels. Macromolecules 1996;29(1):398–406.
[9] Robisson A, Maheshwari S, Musso S, Thomas JJ, Auzerais FM, Han D, et al. Reactive elastomeric composites: when rubber meets cement. Compos Sci Technol 2013;75:77–83.
[10] Spangle LB. Expandable cement composition, vol. US4797159 A. U.S.: Dowell Schlumberger Incorporated; 1986.
[11] Mo L, Deng M, Tang M. Effects of calcination condition on expansion property of MgO-type expansive agent used in cement-based materials. Cem Concr Res 2010;40(3):437–46.
[12] Chatterji S. Mechanism of expansion of concrete due to the presence of dead-burnt CaO and MgO. Cem Concr Res 1995;25(1):51–6.
[13] Cooper W, Grace NS. Elastomers. J Polym Sci Part C: Polym Symp 1966;12(1):133–50.
[14] Dick JS, Annicelli RA. Rubber technology: compounding and testing for performance. Hanser; 2001.
[15] Smithson GL, Bakhshi NN. The kinetics and mechanism of the hydration of magnesium oxide in a batch reactor. Can J Chem Eng 1969;47(6):508–13.
[16] Birchal VS, Rocha SDF, Mansur MB, Ciminelli VST. A simplified mechanistic analysis of the hydration of magnesia. Can J Chem Eng 2001;79(4):507–11.
[17] Rocha SDF, Mansur MB, Ciminelli VST. Kinetics and mechanistic analysis of caustic magnesia hydration. J Chem Technol Biotechnol 2004;79(8):816–21.
[18] Khangaonkar PR, Othman R, Ranjitham M. Studies on particle breakage during hydration of calcined magnesite. Miner Eng 1990;3(1–2):227–35.
[19] Magnesium oxide product data. In: Matthews K, editor. The CRYSTRAN handbook of infra-red and ultra-violet optical materials, Crystran Ltd.; 2012. Available at: http://issuu.com/crystran/docs/handbook?e=2724951/2745150.
[20] Jiang F, Speziale S, Duffy TS. Single-crystal elasticity of brucite, $Mg(OH)_2$, to 15 GPa by Brillouin scattering. Am Mineral 1996;91(11–12):1893–900.
[21] Guth E. Theory of filler reinforcement. J Appl Phys 1945;16(1):20–5.
[22] Lewis TB, Nielsen LE. Dynamic mechanical properties of particulate-filled composites. J Appl Polym Sci 1970;14(6):1449–71.